A&A manuscript no.
(will be inserted by hand later)

Your thesaurus codes are:
01 (09.09.1: M 17; 09.04.1; 09.13.2; 09.01.2; 13.09.3; 13.09.4)

ASTRONOMY
AND
ASTROPHYSICS
28.9.1996

Infrared spectrophotometry of M 17 with ISOCAM*

D. Cesarsky[1], **J. Lequeux**[2], **A. Abergel**[1], **M. Perault**[1], **E. Palazzi**[3], **S. Madden**[4], **and D. Tran**[4]

[1] Institut d'Astrophysique Spatiale, Bat. 121, Université Paris XI, 91450 Orsay CEDEX, France
[2] Observatoire de Paris, 61 Av. de l'Observatoire, 75014 Paris, France
[3] Istituto TESRE/CNR, via Gobetti 101, 40129 Bologna, Italy,
[4] SAp/DAPNIA/DSM, CEA–Saclay, 91191 Gif sur Yvette, CEDEX, France

Received July 1996, accepted sometime later

Abstract. We report spectrophotometric observations of the H II region/neutral medium interface in M 17 obtained with the ISOCAM Circular Variable Filter (CVF) in the spectral range 5.15 to 16.5 μm. The lines of singly–ionized species come mainly from the clumpy "neutral" interface, while the H II region dominates the line emission by higher–ionization species. The emission in the Unidentified Infrared Bands (UIBs) comes from the molecular cloud and the interface and extends into the H II region. In the regions where the radiation field is larger than about 10^4 times the standard interstellar one, the continuum is dominated by the emission of very small grains which are bigger than those responsible for the UIBs.

Key words: ISM: M 17 - ISM: dust - ISM: molecules - ISM: atoms - Infrared: ISM: lines and bands - Infrared: ISM: continuum

1. Introduction

M 17 presents a well–studied case of an interface between an H II region and a neutral molecular cloud. The molecular cloud, M 17 SW lies to the southwest of the H II region and the interface is seen essentially edge–on (Felli et al. 1984). The molecular gas has been extensively mapped in various rotational transitions of CO, CS and other molecules: see in particular the $C^{18}O(2-1)$ maps in Stutzki & Güsten (1990). Far–infrared (FIR) line emission from various neutral and ionized species has been used to study the H II region and the outer regions of the molecular cloud behind the interface where ionizing radiation can penetrate due to its clumpy structure (Stutzki et al. 1988; Meixner et al. 1992 and references herein). The H II region itself is also very clumpy (Felli et al. 1984). Of particular interest is an ultra–compact H II region embedded in the interface, which may represent a second stage of star formation in the complex (Felli et al. 1984). The 3.3 μm Unidentified Infrared Band (UIB) and the adjacent continuum have been studied from the ground by Giard et al. (1992, 1994).

We present here spectrophotometric observations obtained with the ISOCAM long–wavelength camera equipped with Circular Variable Filters (CVF). These observations have allowed a complete mapping of a $3' \times 3'$ field with $6'' \times 6''$ pixels in the wavelength range 5.15 to 16.5 μm. Section 2 describes briefly the observations and reductions; Section 3 reports on the observations of the the ionic lines, while Section 4 describes and interpret the observations of the UIBs and continuum. Section 5 contains the conclusions.

2. Observations and reductions

The observations have been made with ISOCAM on board the Infrared Space Observatory (see Cesarsky et al. 1996a, Kessler et al. 1966 for a complete description). Full scans of the two CVFs of the Long–Wave channel of the camera have been performed in two scanning directions: CVF1 and then CVF2 in increasing wavelength followed by CVF2 and CVF1 in decreasing wavelength. Each wavelength was measured some 40 times in the up–going leg and again another 40 times in the down–going leg. The elementary integration time per measurement was 0.28 seconds. Due to telemetry bandwidth restrictions, four readouts were accumulated on–board before downlinking the data and hence there are 10 independent measurements per pixel per wavelength and per scan leg. The total observing time was 3834 seconds. The effective on–source integration time, i.e. having removed measurements performed while the CVF was stepping, was 3320 seconds.

Send offprint requests to: D. Cesarsky station@iscam1.ias.fr

* ISO is an ESA project with instruments funded by ESA Member States (especially the PI countries: France, Germany, the Netherlands and the United Kingdom) and with the participation of ISAS and NASA.

The pixel size was $6'' \times 6''$; the 32×32 pixel detector covered a total field of view $3' \times 3'$. The effective spectral resolution is of the order of 40. The raw data was processed as follows:

(i) Temporal median filtering of each of the 1024 pixels to remove cosmic ray hits.

(ii) Dark current and flat–field corrections based on the "library" calibration files associated to version 4.3 of the off–line software in Villafranca, Spain.

(iii) Conversion from engineering units to Jy per pixel using again the same calibration data set.

Data for the missing signal from column 24 were interpolated from the adjacent pixels.

The data reduction package is still being optimized to deal with stabilization and transient phenomena. Therefore, no transient corrections were applied nor any read-outs were discarded on account of stabilization considerations. No correction has been made either for zodiacal emission, which is negligible here.

Line strengths presented below have been obtained by summing intensities within an user defined wavelength region and subtracting a mean baseline established from both end positions; the units are then Jy/pixel. This mean baseline is the continuum level at the relevant wavelength. For instance the 16 μm continuum used throughout the text is the baseline of the [Ne III] 15.6 μm line.

Fig. 1 illustrates the dispersion of the measured intensities for pixel [15,15]. There are 161 wavelength samples before data reduction and 145 after having discarded the end points of the CVFs which are still ill–calibrated. The RMS fluctuations of the averaged data for pixel [15,15] are also shown. The mean RMS noise for all 1024 pixels and all 145 wavelength observations is of the order of 5 %.

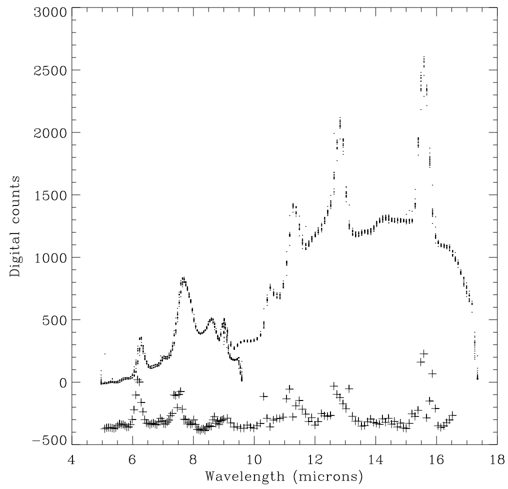

Fig. 1. Example of raw data (pixel [15,15] is illustrated here). Each measured datum is represented by a dot and there are 10 dots per scan leg; the vertical spread at each wavelength gives an idea of both the observation noise and of the reproducibility of the measurement on each leg of the CVF scan. The lower plot shows the RMS fluctuation of the averaged data. Note that the RMS plot has been magnified 10 times and shifted down by 400 units for clarity's sake.

3. Observations of the fine-structure lines

Fig. 2 displays full CVF spectra at three positions, which are identified by circles in the map of Fig. 3 and 5. Position 1 is located in the direction of the H II region and displays the typical IR spectrum of an H II region, with a continuum rising strongly with increasing wavelength and fine–structure lines of [Ar III] 9.0 μm, [S IV] 10.5 μm, [Ne II] 12.8 μm and [Ne III] 15.6 μm. Faint UIBs are also visible at 6.2, 7.7, 8.6 and 11.3 μm. Position 2 is in the direction of the ultra–compact H II region; the same lines are visible as well as relatively stronger UIBs. Position 3 is in the direction of the molecular cloud; it displays a typical UIB spectrum and relatively faint fine–structure lines. The [Ar II] 7.0 μm line is barely visible on these spectra but is quite clear in zoomed displays.

Fig. 3 is a superimposition of maps in the [S IV] 10.5μm and [Ne III] 15.6μm lines. While it is clear that emission in both lines originates from the H II region itself, there are minor differences between their distributions. In fact, weak emission in these lines is present over the whole studied field. An interesting feature is the extension of the

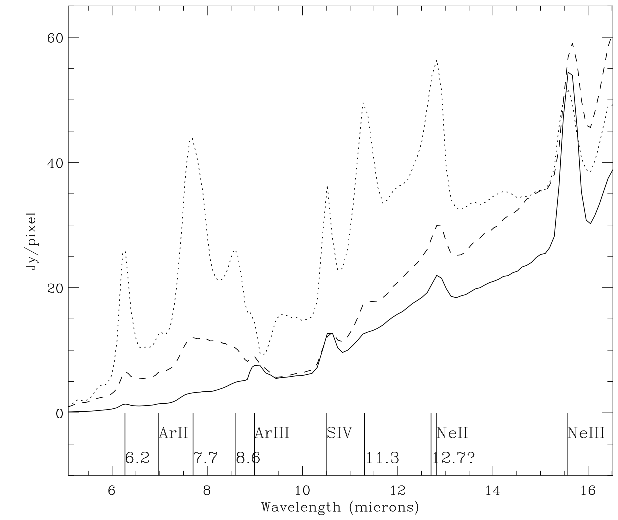

Fig. 2. Full CVF spectra at three positions in the observed field. Pos.1 (solid line) is in the direction of the M 17 HII region, Pos.2 (dashed line) is in the direction of the ultra–compact HII region and Pos. 3 (dotted line, magnified ten times) is in the direction of the molecular cloud (see Fig. 3 for location of lines of sight). The ordinates give Jy/pixel and should be divided by 36 to give Jy per square arcsecond. The fine–structure lines and UIBs are identified.

emission towards α(1950) 18h 17m 34s, δ(1950) -16° 15', which corresponds to ionization by the very reddened O8 star LH 7 (Lemke & Harris 1981).

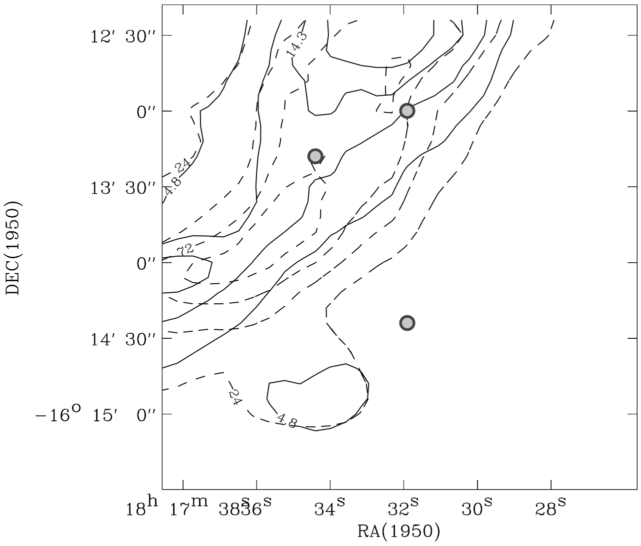

Fig. 3. Superimposition of maps in [SIV] 10.5μm (solid contours) and [NeIII] 15.6μm (dashed contours). The three shaded circles represent, from east to west, positions 1, 2 and 3 referred to in Figure 2.

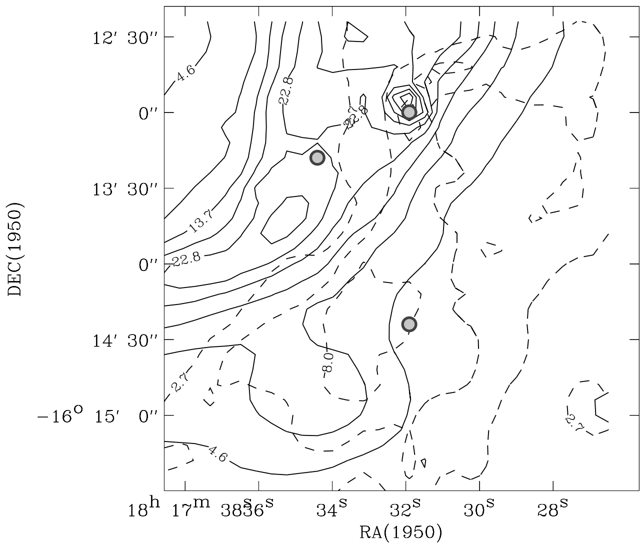

Fig. 4. Map in the 16 μm continuum emission. Superimposed is the map in the 6.2 μm UIB emission (dashed contours). Note the extension of the UIB contours to the left of the continuum map, showing UIB emission inside the HII region.

We have also produced maps of the [Ar II] 7.0μm line (not shown here). This line might be confused with a faint UIB at 6.9μm but the higher–resolution SWS spectra of M 17 taken by Verstraete et al. (1996) show that this effect is negligible at least in the region they have studied. The [Ar II] emission is concentrated around the interface and might extend faintly throughout the whole observed part of the molecular cloud. This is consistent with what has been found for lines of other single–charged ions like Si II or C II , or for the [O I] 63μm and [C I] 610μm lines (Meixner et al. 1992 and references herein). The stronger 12.8 μm feature is a blend of the [NeII] 12.8μm line with an UIB at 12.7 μm (see Verstraete et al. 1996) and its interpretation is ambiguous. One should be suspicious in general of the interpretation of monochromatic maps at this wavelength.

4. The continuum and the Unidentified Infrared Bands (UIBs)

Fig. 4 shows a map of the continuum emission at 16 μm and of the 6.2 μm UIB emission. The 16 μm continuum is strongest near the interface, but is well visible in the direction of the H II region, showing clearly that the emitting grains survive inside H II regions. The distributions in the other UIBs are very similar and are not displayed.

While the UIB and molecular gas distributions show some similarities, there is a conspicuous difference: the band emission extends to the left of the interface, inside the H II region (see also figures 2 and 5). It is clear that the carriers of the UIBs can survive for some time inside the H II region while the neutral gas is ionized by the UV radiation of the exciting stars. A detailed modelling will allow to give the time scale for the destruction of carriers, in the same way as Woodward et al. (1989) have done in the case of the planetary nebula NGC 7027. It will also be interesting to compare the present data with those of Giard et al. (1992, 1994) who have mapped the 3.3 μm band and the adjacent continuum.

In a similar study of the reflection nebula NGC 7023, Cesarsky et al. (1996b) have shown that in this nebula the UIBs are emitted by very small grains heated by single photons (the PAH hypothesis). The band spectra in M 17 are very similar and there can be no doubt that the carriers are the same. Cesarsky et al. (1996b) and Boulanger et al. (1996) have also shown that there is a continuum associated with these carriers in objects where the radiation field is 10 to more than 1000 times the standard interstellar one. The continuum around 10 μm in the direction of the molecular cloud in M 17 (Position 3) can be accounted for entirely in this way, but the continuum at longer wavelengths is already too strong. In the interface and the HII region (Position 1; see also fig. 1 of Verstraete et al. 1996) there is a very intense continuum while the UIBs are relatively fainter. This continuum is that of another population of three-dimensional very small grains

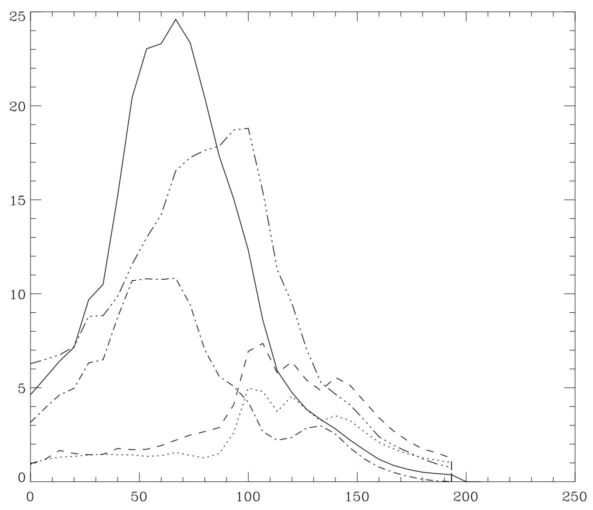

Fig. 5. Continuum and line emission along a direction perpendicular to the ionization front (same direction used by Verstraete et al. 1996). Solid line: 16 μm continuum emission; dash-dot-dot-dot: NeII; dash-dot: SIV; dot: 6.2 μm UIB emission; dash: 11.3 μm UIB emission. Note that the NeII line is clearly contaminated by UIB emission at 12.7 μm. The abscissa is distance in arcsec from RA 18h17m39s; DEC -16°12'54". See Section 2 for an explanation of the intensity units.

(Désert et al. 1990) which start to give a substantial contribution in our wavelength range only if the radiation field is very high: in M 17 it reaches the order of 10^5 times the standard one at the interface (Stutzki et al. 1988).

The spectrum of the ultracompact H II region (position 2) shows several interesting features. First, comparison with the spectrum of M 17 suggests silicate absorption at 9-10 μm. Second, it exhibits a broad, smooth emission instead of the usual well-defined 7.7 and 8.6 μm bands. This feature is similar to that observed in protoplanetary nebulae like IRAS 22272+5435 where the UV radiation field is also extremely strong, and might be attributed to carbonaceous grains similar to terrestrial semi-anthracite (Guillois et al. 1996). Clearly emission by such grains becomes dominant only in regions of extremely high radiation density, but is still negligible in reflection nebulae or the photodissociation region of M 17.

5. Conclusions

We have presented the first high-resolution images of a photodissociation interface in infrared fine–structure lines and in UIBs. We have achieved a resolution of the order of 6″ corresponding to about 0.06 pc at an assumed distance of 2.2 kpc, and comparable to that of the CO(2-1) observations of Stutzki & Güsten (1990). This data base requires detailed modelling for being exploited properly, but some immediate results have been obtained:

1. We confirm that the fine–structure line emission of singly–ionized ionic species is strong at the interface and to some depth inside the molecular cloud, where the UV radiation can penetrate due to its clumpy structure. The emission of higher–ionization species like Ne III and S IV is strong in the H II region itself.
2. The different UIBs are distributed in remarkably similar ways and extend inside the H II region and deep inside the molecular cloud. They are very probably due to PAHs. However a broad feature instead of the 7.7–8.6 μm bands is found in the direction of an ultra–compact H II region and might be attributed to coal grains; this emission dominates only in extremely high radiation fields.
3. While there exists an underlying continuum superimposed on the UIBs and probably due to the same carriers as them (Cesarsky et al. 1996b), another continuum starts to dominate around 15 μm in regions of high radiation field (say more than 10^4 times the standard one). It is probably due to small, three-dimensional grains (Désert et al 1990).

Acknowledgements. We thank the referee, Kris Sellgren, for many relevant comments.

References

Boulanger F., Reach W., Abergel A. et al. 1996, this issue
Cesarsky C. et al. 1996a, this issue
Cesarsky D., Lequeux J., Abergel A., Pérault M., Palazzi E., Madden S., Tran, D. 1996b, this issue
Désert F.-X., Boulanger F., Puget J.-L. 1990, A&A 237, 215
Felli M., Churchwell E., Massi M. 1984, A&A 136, 53
Giard M., Bernard J.-P., Dennefeld M. 1992, A&A 264, 610
Giard M., Bernard J.-P., Lacombe F., Normand P., Rouan D. 1994, A&A 291, 239
Guillois O., Nenner I., Papoular R., Reynaud C. 1996, ApJ 464, 810
Kessler M. et al., 1966, this issue
Lemke D., Harris A.W. 1981, A&A 99, 285
Meixner M., Haas M.R., Tielens A.G.G.M., Erikson E.F., Werner M. 1992, ApJ 390, 499
Stutzki J., Güsten R. 1990, ApJ 356, 513
Stutzki J., Stacey G.J., Genzel R., Harris A.I., Jaffe D.T., Lugten J.B. 1988, ApJ 332, 379
Verstraete L., Puget J.-L., Falgarone E., Drapatz S., Wright C.M., Timmermann R. 1996, this issue
Woodward C.E., Pipher J.L., Shure M., Forrest W.J. 1989, ApJ 342, 860

This article was processed by the author using Springer-Verlag LaTeX A&A style file *L-AA* version 3.